SPECIAL ISSUE

Physical weathering of building stones induced by freeze–thaw action: a laboratory long-term study

J. Ruedrich · D. Kirchner · S. Siegesmund

Abstract Damages to natural building stones induced by the action of frost are considered to be of great importance. Commonly, the frost resistance of building stones is checked by standardised freeze–thaw tests before using. Corresponding tests normally involve 30–50 freeze–thaw action cycles. In order to verify the significance of such measurements, we performed long-term tests on four selected rocks over 1,400 freeze–thaw action cycles. Additionally, numerous petrophysical parameters were analysed to compare the behaviour of rocks in the weathering tests according to the current explanatory models of stress formation by growing ice crystals in the pore space. The long-term tests yield more information about the real frost sensibility of the rocks. A clear deterioration cannot be determined in most cases until 50 weathering cycles have been completed. In the freeze–thaw tests, the samples are also stressed by changing temperature and moisture, indicating that different decay mechanisms can interfere with each other. Thus, thermohygric and moisture expansion are important damage processes.

Keywords Freeze–thaw action · Natural building stones · Microfabric · Pore space properties

J. Ruedrich (✉) · S. Siegesmund
Department of Structural Geology and Geodynamics,
Geoscience Centre, University of Goettingen,
Goldschmidtstr. 3, 37077 Goettingen, Germany
e-mail: jruedri@gwdg.de

D. Kirchner
German Mining Museum, Am Bergbaumuseum 28,
44791 Bochum, Germany

Introduction

Frost weathering was discussed as a major physical deterioration process. Alternating freeze and thaw cycles are probably responsible for most damages in natural building stones during the winter. Numerous freeze–thaw cycles can occur in Central Europe (e.g. in Munich, Germany sometimes over 30 per year).

The causes of ice formation from a solution are widely known. Ice crystallisation processes can be divided into the mechanisms of nucleation and crystal growth. Amongst normal atmospheric conditions, pure water freezes at the 0°C transition. In contrast, water crystallises mostly at a lower temperature than 0°C in porous rocks. The cause can be a super-cooling or a decrease of the freezing point of the fluid. Super-cooling will be generated by the lack of sufficient nuclei (Chahall and Miller 1965). Since in natural stones enough nuclei in the form of crystal surfaces are available, heterogeneous nucleation can be assumed, and thus, only slight super-cooling takes place (Snethlage 1984). In the case of the freeze point reduction, the equilibrium conditions of the fluid have changed. The cause for this could be specific water salinities, which often occurs at buildings. However, the main cause for the freeze point reduction in natural building stones is the pore space distribution. The smaller the pore, the stronger the water is strained, and therefore freezing at increasingly lower temperatures results. Since natural building stones show a wide range of pore sizes (Fitzner and Snethlage 1982), a heterogeneous crystallisation occurs during cooling. Whereas in larger pores water is already crystallised, the water in smaller pores can still be in a liquid state. Of crucial importance are also further pore space properties such as the shape (Hirschwald 1908) and the interconnection of pores (Stockhausen 1981; Weiss 1992).

The mechanism whereby ice crystallisation generates stresses within the rock fabric is still under discussion. For a long time, the volumetric expansion of pore water upon freezing (9 vol.% under atmospheric conditions; Hirschwald 1908) was held responsible for the formation of stress within the rock fabric. However, many observations contradict this supposition (e.g. Walder and Hallet 1985). Many authors support the theory that the movement of water from smaller pores or unfrozen areas to growing ice crystals in larger pores lead to the formation of stresses by capillary (Everett 1961) and hydraulic (Powers and Helmuth 1953; Setzer 1999) pressures. Furthermore, the linear growth pressure, introduced by Correns and Steinborn (1939), was discussed as the main process of stress development within the rock fabric (Scherer 1999; Steiger 2005; Ruedrich and Siegesmund 2007). Hence, the basic precondition for the development of damages due to frost action is that the stresses induced by ice crystallisation exceed the strength of the rock (Winkler 1968).

To check the frost resistance of building materials, standard freeze–thaw tests are used. The samples are cyclically loaded by cooling in a freezer and thawing in warm water. After a certain number of cycles, the sample changes were checked by measuring the loss of weight and noting the presence of any macroscopic damages. Due to economic reasons, only a few freeze–thaw cycles were performed. In many cases, the investigations lead to the conclusion that frost action tests activate the main rock discontinuities, like pre-existing cracks (e.g. partially mineralised) or the sedimentary bedding (e.g. Nicholson and Nicholson 2000; Thomachot and Jeanette 2002). Based on this conclusion, many authors do not attach great importance to the total fabric decay by frost action processes.

In order to verify the significance of such tests, long-term investigations were carried out. This work presents the results on four different actual building stones: a limestone from Kuaker, a porphyry from Lobejuen, a granite from Knaupsholz and a tuff from Habichtswald. All the mining sites are located in Germany. These rocks are part of a comprehensive investigation programme using more than 20 different rock types. The present work shows the first results of this research. The rocks were chosen because of their different behaviours in the freeze–thaw tests. The rock samples were subjected to 1,400 freeze–thaw cycles. To acquire more information about the dependence of weathering on the rock fabric, the results were compared with different petrophysical properties. For this purpose, the pore space properties (porosity and pore radii distribution), the water transport and restore properties (capillary water uptake, water diffusion resistance and saturation degree), the tensile strength and the moisture as well as thermal expansion properties were investigated.

Additionally, length change measurements during freezing under dry and water-saturated conditions were performed to acquire more information about the damage mechanisms of single freeze–thaw cycles. Length change measurements are a useful tool for this purpose (Thomachot and Matsuoka 2007).

Investigated rocks

Fabric properties

The Kuaker Kernstein (Fig. 1a) is a biogenic limestone from the lower Triassic (Bavaria, Germany) and can be classified as floatstone. The mineralogical composition is dominated by calcite between 92 and 98%. Accessory clay minerals and iron oxide as well as hydroxide minerals occur. The limestone shows a clear bedding of alternating shell-rich and matrix-dominated layers. Sparitic grain fabrics are common in the shell-rich layers (Fig. 2a). The shell fragments are made of sparitic grains which are covered with a micritic margin. Shell fragments can reach sizes up to several millimetres. The cement, which preferentially fills the pore spaces of the shell fragments, also exhibits sparitic grain sizes between 160 and 400 μm. This cementation leads to a strong reduction of the pore space. In sparitic areas, the calcite crystals typically show polygonal grain shapes with more or less straight grain boundaries. Fe- and Mn-covers or crusts at grain boundaries are often observable in the shell-rich layers. They cause the yellow brown colour in these areas. The matrix-dominated layers of the limestone are rarer and are made of a very fine-grained micritic fabric.

The rock from Lobejuen is rhyolitic in composition and characterised by a typical porphyritic fabric (Fig. 1b). The age of this volcanic rock is dated at the boundary of the Upper Carboniferous and Lower Permian. The rock forms part of a volcanic complex near Halle (Saxony-Anhalt, Germany). In the fine-grained red matrix idiomorphic crystals of plagioclase, alkali feldspar and quartz are common (Fig. 2b). The fine-grained matrix consists predominantly of quartz and subordinated alkali feldspar. Accessory biotite and chlorite also occur. The grain sizes of the matrix minerals are less than 50 μm. The porphyritic minerals achieve grain sizes up to 20 mm. Microscopically, the feldspar inclusions often show sericitic alteration. Commonly, quartz shows idiomorphic to hypidiomorphic single crystal shapes, but it also occurs as polycrystalline quartz aggregates. Biotite is often altered to chlorite. Haematite appears as a finely dispersed pigment in the matrix, which causes the red colour of the rock.

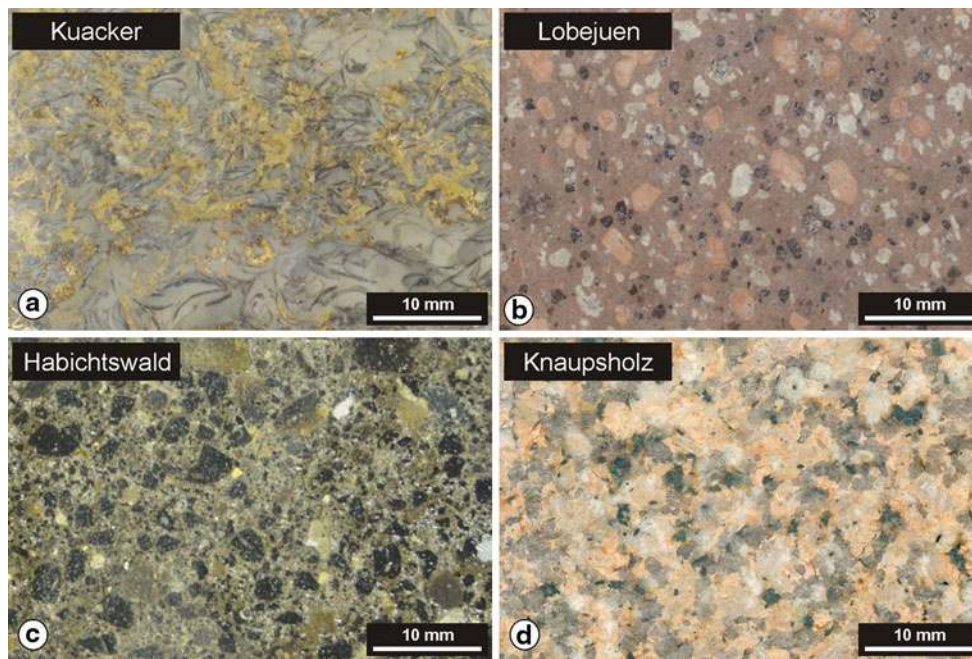The Miocene volcanic rock from Habichtswald (Hessen, Germany) represents a lapilli tuff of basaltic composition

Fig. 1 Macrofabrics of the investigated rocks: **a** Kuaker limestone, **b** Lobejuen porphyry, **c** Habichtswald tuff and **d** Knaupsholz granite
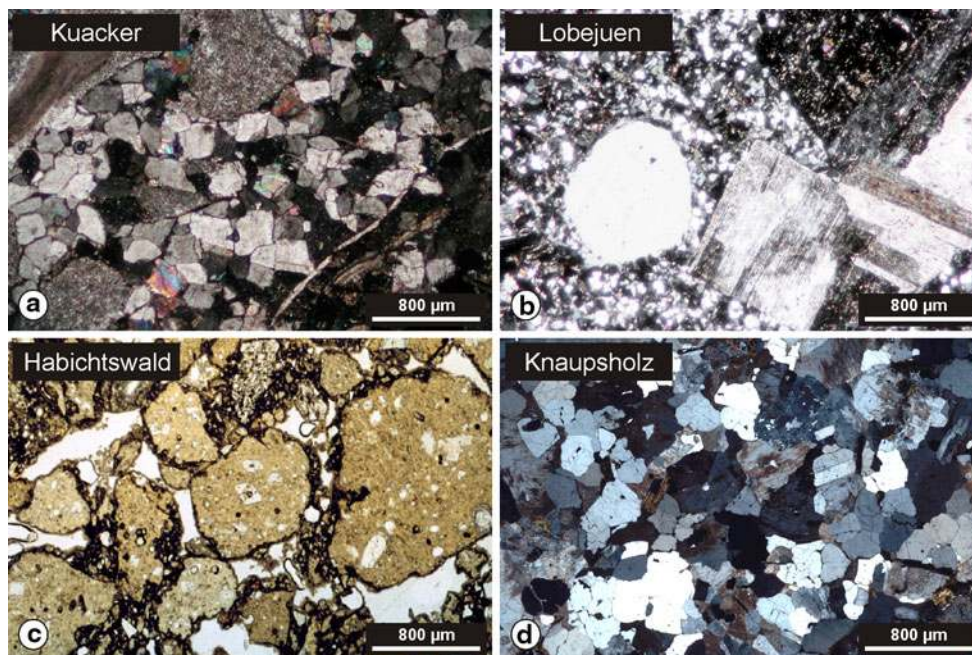

Fig. 2 Microfabrics of the investigated rocks (crossed polariser): **a** sparitic fabric of the Kuaker limestone, **b** Lobejuen porphyry, **c** lapillus in a hyaline matrix of the Habichtswald tuff and **d** quartz area of the Knaupsholz granite

(Fig. 1c). The lapilli fragments with sizes between 0.5 and 15 mm are embedded in a fine-grained and partly hyaline groundmass (Fig. 2c). In this heterogeneous matrix, pyroxene and olivine are dominant, and subordinated biotite and hornblende occur. The lapillus consists of highly porous solidified lava fragments or pumice. The shapes of the fragments are mostly polygonal and partly rounded.

Subordinate xenolithic enclosures of predominantly red sandstone also occur. The pore space is very heterogeneous. Beside macroscopic pores in the range of millimetres also micropores in the heterogeneous fine-grained matrix occur.

The rock from Knaupsholz (Harz Mountains, Saxony-Anhalt, Germany) is a slight to medium altered granite

Table 1 Pore space and density properties of the investigated rocks in non-weathered condition

Rock type	Porosity (vol.%)	Bulk density (g cm^{-3})	Particle density (g cm^{-3})	Average pore radius (μm)	Pore radii distribution (%)				
					0.001–0.01 (μm)	0.01–0.1 (μm)	0.1–1 (μm)	1–10 (μm)	>10 (μm)
Kuaker	3.73	2.68	2.75	0.050	23.2	44.2	22.8	7.6	2.2
Lobejuen	4.52	2.52	2.64	0.040	12.0	73.3	10.7	2.7	1.3
Habichtswald	20.87	2.14	2.71	0.033	53.3	18.9	14.6	7.2	6.0
Knaupsholz	1.83	2.58	2.63	0.108	10.9	39.6	34.7	14.8	0.0

showing a greyish red colour (Fig. 1d). This plutonic rock is dated as Upper Carboniferous, which corresponds to the end of the Variscan orogeny. Microscopically, the rock shows a granular grain fabric (Fig. 2d). The grain size of the coarser fraction is about 0.5 cm. The main mineral phases of the rock are 55% feldspar, about 40% quartz and 5% biotite. Accessory magnetite and zircon are observable. The feldspar minerals are partly characterised by a strong sericitisation. Biotite is commonly altered to chlorite. Polycrystalline aggregates of quartz often show deterioration by inter- and intragranular microcracks.

Petrophysical properties

The mineralogical composition and fabric determine the petrophysical properties of the rocks. Due to the pronounced fabric differences of the investigated rocks, their petrophysical properties also vary greatly. Except for the pore space investigations, all petrophysical analyses were performed in three orthogonal directions. A reference coordinate system, with respect to the macroscopically visible elements of foliation and lineation, was chosen. The XY-plane marks a foliation or sedimentary bedding, while the X-direction is parallel to the lineation (if present). An arbitrary coordinate system was defined if the specimens did not show the respective macroscopically visible fabric elements.

To characterise the total accessible porosity (Φ), measurements of hydrostatic weighting were performed on sample cubes (65 × 65 × 65 mm). The dry (m_{dry}), the saturated (m_{sat}) and the hydrostatic mass (m_{hydro}) of the saturated samples were determined. Total water saturation was obtained by using a vacuum. Porosity was calculated by $\Phi = m_{sat} - m_{dry}/m_{sat} - m_{hydro} \times 100$. The investigated samples show a wide range of porosity, caused by their different geological origins. They vary between 1.83% for the Knaupsholz Granite and 20.87% for the Habichtswald Tuff (Table 1). From the mass values, the bulk ($\rho_{bulk} = m_{dry}/m_{sat} - m_{hydro}$) and particle density ($\rho_{particle} = m_{dry}/m_{dry} - m_{hydro}$) was also calculated (Table 1). The particle densities correlate with the densities of the dominant minerals in the respective rock. The rocks from

Lobejuen and Knaupsholz exhibit densities between 2.63 and 2.64 g cm^{-3} which is more or less the mineral density of quartz and feldspar. The Habichtswald rock shows a high particle density caused by the high amount of mafic minerals. The highest particle density of 2.75 g cm^{-3} was observed in the Kuaker limestone, which is higher than the mineral density of calcite (2.72 g cm^{-3}). The reason for this could be a certain fraction of dolomite (2.87 g cm^{-3}) or the influence of the clay mineral content. The Kuaker limestone also shows the highest bulk density. The lowest bulk density is detectable in the Habichtswald rock and is caused by its high porosity.

The pore size distribution of the rocks was determined by using mercury porosimetry (van Brakel et al. 1981). The investigations were carried out with pressures up to 2 kbar, which allows the evaluation of pore radii of about 0.005 μm. At least three specimens (⌀ 12.5 × 20.0 mm) of every rock type were analysed. The results show comparable distributions for the respective rock type. The data in Table 1 represent results of single measurements.

The investigated rocks show a broad spectrum of pore radii distributions (Table 1). All samples are characterised by a large amount of micropores below 0.10 μm. Based on this, the average pore radius is also equal or lower than 0.11 μm (Table 1).

In order to constrain the directional dependence of capillary water absorption analysis, the sample cubes (65 × 65 × 65 mm) were cut according to the three principal directions (X, Y, Z) of the reference coordinate system. Thus, directionally dependent measurements could be detected on one sample. The specimens were dipped into about 0.3 cm of water. For data acquisition, an underfloor scale was used with digital recording of the weight increase (m_{cap}) every minute. The water absorption coefficient (w-value) was calculated from the weight increase per unit area versus the square root of the time (w-value = $m_{cap} A^{-1} t^{-1/2}$). The w-value of the investigated rocks varies between 0.17 kg m^{-2} h$^{-1/2}$ for the Z-direction of the Lobejuen porphyry and 2.49 kg m^{-2} h$^{-1/2}$ parallel to the X-direction of the Habichtswald Tuff (Table 2).

The water vapour diffusion resistance value (μ) of the sandstones was studied using the wet-cup method

Table 2 Moisture transport and restore properties of the investigated rocks in non-weathered condition (anisotropy calculated with $A = n_{max} - n_{min}/n_{max} \times 100$)

Rock type	w-value (kg m^{-2} h$^{-1/2}$)			A (%)	μ-value			A (%)	S-value
	X	Y	Z		X	Y	Z		
Kuaker	0.35	0.25	0.20	42.9	277.87	147.19	449.21	67.2	0.71
Lobejuen	0.19	0.19	0.17	10.5	98.76	92.37	104.86	11.9	0.81
Habichtswald	2.49	2.32	1.99	20.1	20.25	17.41	19.87	14.0	0.84
Knaupsholz	0.39	0.34	0.39	12.8	146.49	172.66	141.91	17.8	0.78

(Poschlod 1989) on disc-shaped samples ($\varnothing$ 40 × 10 mm). μ characterises the diffusion resistance of a porous material compared to an equally dimensioned inactive air film. Slices of the stones were attached as covers on Teflon cups. The relative humidity on the outside and inside of the cups was different. This causes moisture to flow through the porous material from the side with higher (inside 100%) to the side with lower relative humidity (outside 50%). The moisture flow was obtained by weighing the cups at various times. Besides capillary absorption, the diffusion of water vapour is the second most important water transport mechanism in porous materials. The non-dimensional water vapour diffusion resistance value (μ), which is normally used to describe the measure of water vapour diffusion, is lowest for the Habichtswald rock with 17.41 parallel to the Y-direction. In contrast, the limestone from Kuaker shows the highest vapour diffusion resistance with 449.21 perpendicular to the bedding (Table 2).

The water saturation degree (S-value) describes the voluntary water absorption of a rock under atmospheric conditions. The measurements were carried out on the same cubic samples as those used for porosity measurements. The S-value was determined by dipping the samples in water for 24 h. Afterwards, the samples were totally immersed for another 24 h. The S-value is for most of the investigated rocks medium between 0.72 and 0.81. Only the saturation degree of the Habichtswald Tuff with 0.84 nearly reaches the critical value of 0.90 (Hirschwald 1908). This critical value arises from the fact that the volume expansion induced by the phase transition from water to ice is around 9 vol.% under atmospheric conditions. Based on this, a porous rock with more than 91% water content could sustain direct frost damage. Thus, rocks with a saturation degree of voluntary water absorption of more than 90% (S-value of 0.9) should be extremely vulnerable to frost action (Hirschwald 1908).

The tensile strength (σz) was determined by means of the "Brazilian test", which involves disc-shaped specimens ($\varnothing$ 40 × 20 mm). In order to calculate the average value, a minimum of four samples was used. A constant strain rate of 0.3×10^{-6} mm s^{-1} ($\approx 10^{-5}$ s^{-1}) was applied. The

Table 3 Tensile strength of the investigated rocks in non-weathered condition

Rock type	Tensile strength			
	$\perp XY$ (N mm^{-2})	$\perp XZ$ (N mm^{-2})	$\perp YZ$ (N mm^{-2})	A (%)
Kuacker	5.27	5.73	5.53	8.3
Lobejuen	8.65	10.69	11.86	27.1
Habichtswald	2.52	3.28	2.16	34.2
Knaupsholz	4.81	6.07	5.73	20.8

tensile strength was measured perpendicular to the XY-, XZ- and YZ-planes. The resistance of rocks against tensile stresses is an important parameter for frost weathering processes because the induced stresses by crystallisation have to exceed the tensile strength before damage occurs. The tensile strength varies for the different rock types between 2.16 N mm^{-2} perpendicular to the YZ-plane for the Habichtswald Tuff and 11.86 N mm^{-2} perpendicular to the same direction for the Lobejuen rock (Table 3).

The thermal expansion behaviour was measured on cylindrical samples ($\varnothing$ 15 × 50 mm). The directional dependence of the thermal expansion was determined as a function of temperature using a dilatometer with six measuring sets. The final displacement resolution was better than 1 μm. Samples were subjected to a thermal heating cycle from 20 up to 90°C and back to the initial temperature. From the experimentally determined temperature and dilatation data, the coefficient of thermal expansion was calculated using the relation $\alpha = \Delta l/l \times \Delta T$. Furthermore, the residual strain was determined after the heating cycle. For a detailed description of the experimental setup refer to Koch and Siegesmund (2001). The thermal expansion coefficient α expresses the expansion of a material as a function of temperature. The rocks from Habichtswald and Knaupsholz show relatively low thermal expansion coefficients with an average value of around 7.2×10^{-6} K^{-1} (Table 4). The highest value is observable for the rock from Lobejuen with an average value of 8.5×10^{-6} K^{-1}. The Kuaker limestone exhibits a medium

Table 4 Thermal expansion coefficients (α) and the residual strain of one heating cycle (20°C–90°C–20°C) as well as the hygric expansion of the investigated rocks in non-weathered condition

Rock type	Thermal dilatation					Hygric expansion			
	X (10^{-6} K^{-1})	Y (10^{-6} K^{-1})	Z (10^{-6} K^{-1})	A (%)	Residual strain (mm m^{-1})	X (mm m^{-1})	Y (mm m^{-1})	Z (mm m^{-1})	A (%)
Kuacker	6.64	7.91	8.20	19.0	0.04	n.d.	n.d.	n.d.	–
Lobejuen	8.57	7.93	9.02	12.1	n.d.	0.06	0.07	0.06	14.3
Habichtswald	7.43	6.95	7.19	6.5	n.d.	0.12	0.15	0.12	20.0
Knaupsholz	6.92	–	7.49	7.6	n.d.	0.26	0.30	0.19	36.7

n.d. not detectable

value of around 7.6×10^{-6} K^{-1}. This material shows the highest anisotropy of the thermal expansion coefficient with a value of 19% for the investigated rocks (Table 4).

After one heating cycle, the Kuaker limestone shows a pronounced residual strain of 0.04 mm m^{-1}. This behaviour is evidence for a thermal deterioration due to microcracking. For the other rocks, no residual strain is detectable after thermal heating.

The moisture expansion of the rocks was determined on cylindrical samples (∅ 20 × 50 mm), which were pre-conditioned at 30% relative humidity and room temperature. Afterwards, the samples were completely immersed in distilled water. The accuracy of the displacement transducer is 1.0 µm. The investigations were carried out on samples parallel to the X-, Y- and Z-directions. For the investigated samples, large differences of moisture expansion were observable (Table 4). Whereas the limestone from Kuaker shows no swelling, the samples from Lobejuen and Habichtswald exhibit a slight medium moisture expansion between 0.06 and 0.15 mm m^{-1}. Only the Knaupsholz Granite showed a remarkably large swelling of 0.30 mm m^{-1} parallel to the Y-direction. This phenomenon is possibly caused by the medium alteration of this rock with the formation of cracks and clay minerals.

Freeze–thaw weathering tests

In order to verify the sensitiveness of the rocks against freezing, freeze–thaw tests were performed in the laboratory. Rock prisms with a dimension of 40 × 40 × 160 mm were tested. Two specimens were examined for each rock type, which show comparable behaviour. The examination of material deterioration was carried out by measurements of the rod waves (Rentsch and Krompholz 1961). This method allows the evaluation of the compressional wave velocities (V_p) and the dynamic Young's modulus (dE). The measurements were carried out parallel to the long axis of the sample perpendicular to the bedding/foliation (Z-direction). Furthermore, the sample weight was measured. For one test

cycle, the samples were first immersed in water at a temperature of 20°C for 2 h. Afterwards, the samples were stored in a special freezer at −20°C for 16 h. In total, the samples were subjected to 1,400 freeze–thaw cycles. The measurements of material changes were carried out after every 5th cycle until the 350th freeze–thaw cycle was reached, and afterwards every 10th cycle. For this, the samples were dried to weight constancy at 60°C in a drying chamber. Different patterns for the loss of weight and the change of elastic properties are observable, whereas the V_p and Young's modulus generally show a comparable behaviour (Fig. 3). The damage phenomena of the loaded samples are quite different (Fig. 4).

For the Kuaker Limestone, only slight changes of weight are observable (Fig. 3a–c). After 1,400 cycles, only 1% loss in weight was detectable. In contrast, the sample exhibits a large and still consistent decrease of V_p and the Young's modulus. V_p is reduced primarily from 5.8 to 2.4 km s^{-1}. The Young's modulus decreased from a value near 60 to 10 kN mm^{-2}. Damages of the sample are largely lacking, which correlates with the constant weight. Only a distinct macroscopic crack shows progressive opening (Fig. 4a).

The sample from Lobejuen stays more or less unaffected during the freeze–thaw test (Fig. 3d–f). Only the elastic properties show a slight decrease, which is more pronounced in the first 50 freeze–thaw cycles. For the whole test run, only a reduction of the Young's modulus from 55 to 44 kN mm^{-2} could be determined. Even after 1,400 freeze–thaw cycles, no macroscopic damage occurs (Fig. 4b).

In contrast to the other samples, the tuff from Habichtswald shows a strong loss of material (Fig. 3g–i). At the 1,055th freeze–thaw cycle, the sample collapsed. Up to this cycle, the loss of weight amounts to about 7% of its initial value. The V_p values decrease around 50%. The Young's modulus is relatively low in this sample and has a value of 9 kN mm^{-2}. This is caused by the highly porous fabric. It decreases close to 0 kN mm^{-2} up to the break down cycle of the sample. The decrease of the Young's modulus as
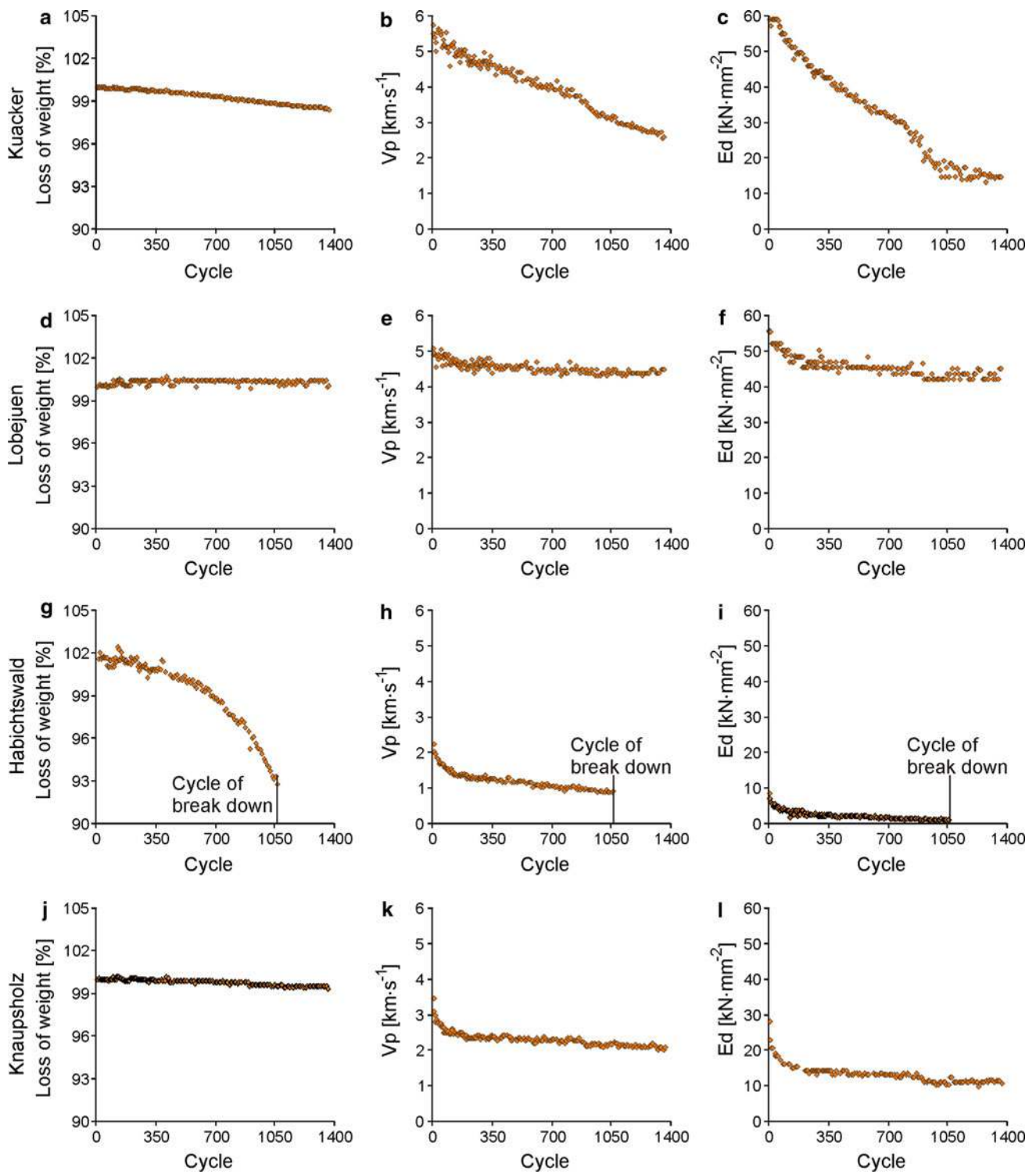
Fig. 3 Results of the standard freeze–thaw test: **a**, **d**, **g**, **j** loss of weight; **b**, **e**, **h**, **k** changes of V_p; **c**, **f**, **i**, **l** changes of the Young's modulus

well as V_p is strong during the first 100 cycles. In the following freeze–thaw cycles, the decrease of V_p is moderate to slight. The tuff shows a strong decay in the form of local breakouts and a crumbling of lapilli fragments (Fig. 4c).

The Knaupsholz Granite shows a different pattern of the measured parameters during the test (Fig. 3j–l). Whereas the weight is more or less constant over the complete test runs, the elastic values show a downgrade. V_p is reduced from 3.5 down to 2.1 km s^{-1}. The Young's modulus shows

Fig. 4 Damage phenomena after 1,400 freeze–thaw tests: **a** distinct crack growth of the Kuaker sample, **b** no damages are observable for the Lobejuen porphyry, **c** strong loss of material of the Habichtswald sample and **d** slight sugar-like crumbling at the edges of the Knaupsholz specimen
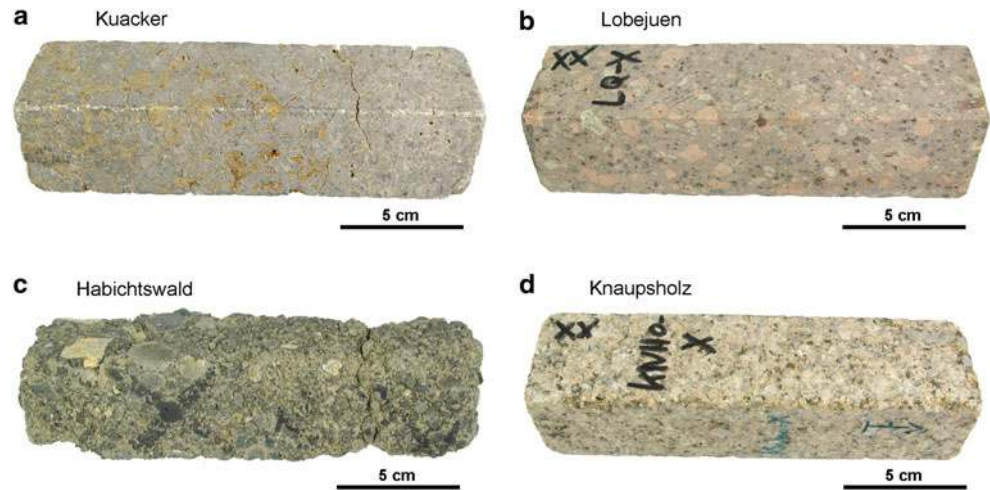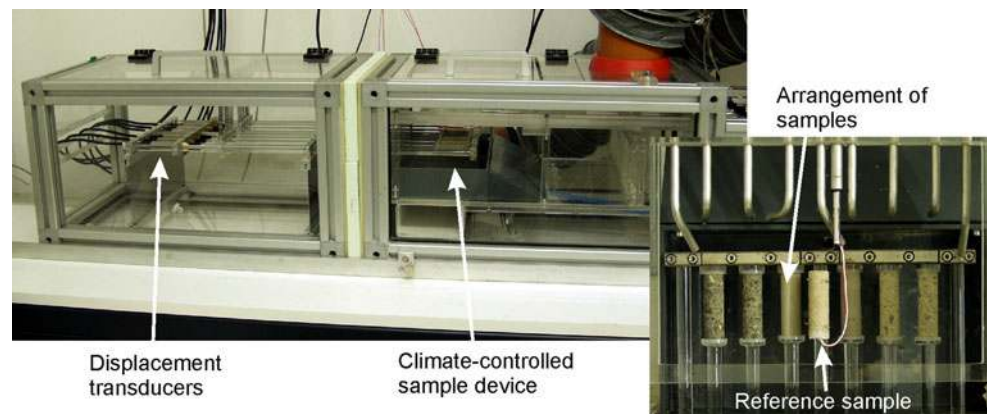

Fig. 5 Dilatometer with climate controlled sample box for the length change measurements of porous solids during frost action

a decrease from about 29 to 8 kN mm^{-2}. For both elastic values, the strongest surge is observable until the 100th freeze–thaw cycle. For the subsequent cycles, only a slight decrease is measurable. Macroscopically, the loaded sample only shows marginal damages in the form of a sugar-like crumbling of single crystals along the specimen edges (Fig. 4d).

Length change induced by freeze–thaw action

To provide detailed information about the weathering mechanisms of ice crystallisation within the pore space, simultaneous length change measurements during frost action were applied. The measurements were carried out in a specially designed dilatometer (Fig. 5). The length change behaviour was determined on cylindrical specimens ($\varnothing$ 15 × 100 mm) in two fabric directions: parallel (X-direction) and perpendicular (Z-direction) to the bedding. To avoid moisture changes within the samples, the specimens were sealed with foil during the experiments. A

reference sample was used to detect the sample temperature. The samples were measured for the experiments in three dry cycles followed by ten cycles under water-saturated conditions. In Fig. 6, the first dry and the first wet cycle are shown. Solution absorption during a wet sample condition takes place through capillary water uptake over 24 h. The specimens were cooled from 20 down to −20°C and heated back to the initial temperature. The temperature steps were held for 6 h each, respectively. The test was carried out with a cooling rate of 0.5°C/min. Due to the different measuring setup between the length change and the freeze–thaw tests, the comparability of the results is limited.

Under dry conditions, the samples show a more or less linear length change when cooling to −20°C as well as during subsequent heating up to 20°C (Fig. 6e–h). After returning to the initial temperature, no residual strain develops, and thus, no damage occurs. The length change behaviour by cooling of water-saturated specimens differs to that of the dry samples. For this purpose, three phenomena are distinguishable:
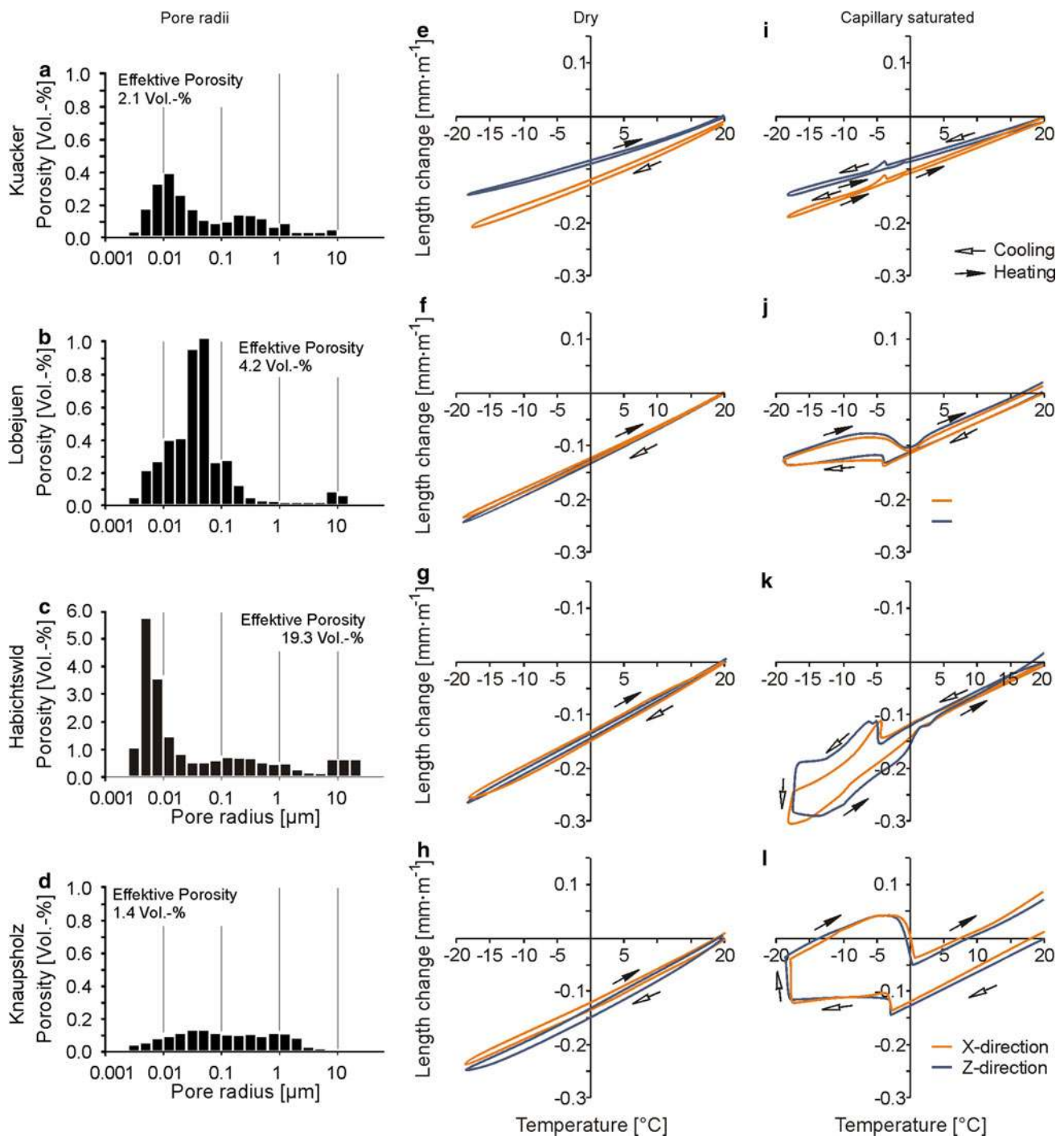
Fig. 6 Pore radii distribution and length change during freeze–thaw action of samples parallel (X) and perpendicular (Z) to the bedding/foliation: a, c dry and b, d water-saturated condition of the samples from a, e, i Kuaker, b, f, j Lobejuen, c, g, k Habichtswald and d, h, l Knaupsholz

1. The differences of intensity between the dry and the wet length change path are a measure of the mechanical stresses within the rock fabric induced by ice crystallisation.
2. The general length change pattern provides information about the interaction between the crystallisation processes and the rock fabric.

3. The residual strain is a dimension of crack growth and thus of the fabric decay.

The length change modification is different for the rock samples investigated. The rock from Kuaker only exhibits a slight length change, whereas the rocks from Lobejuen, Habichtswald and Knaupsholz show a strong modification

of length change between dry and capillary water-saturated conditions (Fig. 6e–l). This is a first indication that ice crystallisation in pore spaces of the latter samples lead to stronger stresses in the rock fabric.

Concerning the pattern of length change for all samples, a general contraction of samples is observed during cooling with a slight expansion at about −4°C. The expansion phenomenon may be traced back to an initial ice crystallisation within the pore space. During subsequent cooling of the samples, two totally different phenomena are observable, which are best discernable for the samples from Habichtswald and Knaupsholz. The Habichtswald Tuff shows a slight contraction between −8 and −18°C. At a temperature equilibration of about −19°C, the tuff is characterised by a strong decrease of length (Fig. 6k). This "frost shrinking" can be traced back to different processes, which may overlie each other. First, a pressure solution of exiting ice crystals by subsequent cooling occurs, and thus, the inverse process of linear growth pressure develops (Correns and Steinborn 1939). This effect can arise if the supercooled water is more or less depleted (Ruedrich and Siegesmund 2007). Furthermore, a buffering effect of the temperature by the large amount of unfrozen water in this sample could be a reason (about 20 vol.% porosity). The further cooling of the sample can only take place until all the water is frozen. The third cause may be a movement of unfrozen water from small pores to ice crystals in larger pores (Everett 1961). With the dewatering of small pores, the swelling effect will be reduced, and the rock shows in combination with the pressure solution of existing ice crystals a shrinking (Ruedrich and Siegesmund 2007). However, this length change pattern was cited in the literature for sandstones (Ruedrich and Siegesmund 2006), and thus, this behaviour seems to be typical for materials with higher porosities and complex pore shapes.

In contrast, the Knaupsholz Granite shows following the length increase at −4°C a further slight expansion during subsequent cooling. During the temperature equilibration phase at about −19°C, a strong expansion occurs. This length change pattern is also observable for the Lobejuen Porphyry. For both rocks, microcracks should represent the main pore space shapes. Thus, differences of the ice crystallisation behaviour within the respective pore geometries may be the cause for the different length change patterns.

Also the residual strain after the freeze–thaw cycle differs for the investigated rocks (Fig. 6i–l). Whereas the sample from Kuaker returns to its initial length, the samples from Lobejuen and Habichtswald show a very slight residual strain. Only the granite from Knaupsholz shows a pronounced residual strain at achieving the initial temperature. This partly contradicts the observations from the freeze–thaw long-term test.

A pronounced anisotropy of length changes is only observable for the rock from Kuaker. This directional dependence may be caused by two specific effects. First, the bedding of this sediment by the shape-preferred orientation of grains or shell fragments as well as pores can generate the observed anisotropy. Second, a preferred crystallographic orientation (texture) of the calcite crystals could also be the main reason.

Discussion

For the durability of natural building stones against ice crystallisation processes, the solid body and the pore space is especially important. The solid body is determined by its structure and the interlocking of the crystals. These fabric parameters control the resistance against stress development in the pore space of the material. By its size, shape and interconnection, the pore space controls the amount and distribution of moisture in the rock body, and hence the possibility of ice crystallisation from the solution.

Different mechanisms can contribute to the stress development by ice crystallisation. On the one hand, there is the pure volume expansion during the transition from water to ice (Hirschwald 1908). On the other hand, the linear growth pressure (Steiger 2005) can play an important role, especially at lower water saturation degrees. Furthermore, during crystallisation, water redistribution processes in the pore space can also lead to increasing stresses (Everett 1961; Setzer 1999).

The freeze–thaw tests show that an assessment of the resistance of rocks against ice crystallisation in their pore spaces is possible. But the evaluated data are also evidences that more detailed information can only be determined by long-term measurements. For most of the investigated stones, an early reaction of freeze–thaw action is detectable. However, only after more than 50 freeze–thaw cycles, there is a clear tendency of damage development if the process leads to a total deterioration or only to a slight reduction of the elastic properties.

When comparing the rock properties with their resistance, and accordingly their sensibility in the freeze–thaw test, some conclusions about the reasons and working mechanisms can be drawn. According to the radius freeze point relation after Stockhausen (1981), water should freeze down to pore sizes larger than 0.006 μm at temperatures of −20°C. Thus, within our freeze–thaw test, the water in almost all the pores of the investigated samples could freeze, which is exemplarily shown in Fig. 7 for the Habichtswald Tuff.

During the frost action test, the Kuaker Limestone showed a slight decrease in weight but a strong decrease in the V_p and the Young's modulus. The porosity is low, and
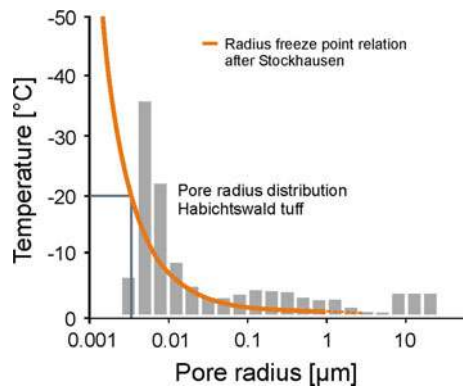
Fig. 7 Radius freeze point relation after Stockhausen (1981)

the tensile strength achieves a medium value for the investigated rocks. The main pore size is about 0.01 μm with a small amount of pores between 0.1 and 1.0 μm. Thus, specific frost sensitivity cannot be expected from the petrophysical properties. However, the strong decrease of the compressional wave velocities is evidence for a pronounced decohesion of the material along the microcracks. A comparable behaviour is known for marbles during weathering (Siegesmund et al. 2008). Calcite rocks are known to exhibit a strong sensibility against changes in the temperature. This is evidenced by the observed residual strain of the Kuaker limestone from the thermal dilatation experiments. Based on this, additional analyses of the hydrothermal expansion behaviour were performed. These tests were carried out at dry and wet sample conditions comparable to a standard marble dilatation test (Siegesmund and Ruedrich 2008) only on samples of the Kuaker limestone. Samples were cyclically heated from 20 up to 90°C and back to the initial temperature. Five dry cycles were followed by ten cycles under wet sample conditions. The tests show that the Kuaker Limestone is characterised by a pronounced sensibility against thermal expansion processes, especially in wet conditions (Fig. 8). After only five dry and ten wet heating cycles, the limestone sample shows a pronounced residual strain up to 1.2 mm m^{-1}. This can be traced back to its partially sparitic fabric in

combination with a strong anisotropic dilatation behaviour of the calcite single crystal. Calcite shows during heating a positive dilatation parallel to the c-axis ($\alpha = 19.2 \times 10^{-6}$ K^{-1}), whereas the crystal contracts parallel to the a-axis ($\alpha = -3.2 \times 10^{-6}$ K^{-1}; Fei 1995). This directional dependence of dilatation leads to stresses within the fabric during changing temperatures. The decay process is progressive, especially if water is present. Since the samples are subjected to temperature and humidity changes in the freeze–thaw test, the thermohygric decay processes should also play an important role.

During the freeze–thaw test, the Lobejuen Quartz Porphyry shows no changes of weight and only a very slight decrease of V_p and the Young's modulus. Also in the dilatation test, no significant residual strain occurs. Only the differences of the length changes between dry and wet sample conditions evidenced mechanical stresses. One cause for the frost resistance of this material should be the pore size distribution. The pore radii show a narrow spaced range between 0.1 and 0.01 μm (Fig. 6b). Only a few pores are above and below this range. This means that the entire water in the pores will freeze in a more or less short temperature range. Thus, only a very slight portion of the unfrozen water in smaller pores can serve as a fluid reservoir for further crystal growth in larger pores. Due to the low porosity, the Lobejuen rock exhibits further a good fabric cohesion. This is also shown by the high value of the tensile strength. Therefore, this material exhibits a pronounced resistance against stresses, which will be induced by ice crystallisation processes within the rock fabric.

The tuff from Habichtswald represents the most sensitive rock in the frost action test measured in this study. The rock is characterised by a high porosity and a low tensile strength. Moreover, the rock has a critical pore space distribution. Besides a large amount of micropores, the rock also shows larger pores in the range above 1 μm (Fig. 6c). In this case, water from small pores can diffuse towards growing ice crystals in larger pores. Hence, if a high amount of small pores are connected to larger pores, a voluminous reservoir for growing ice crystals exists

Fig. 8 Length change during heating of the Kuaker Limestone: **a** first dry cycle, **b** first wet cycle and **c** increasing residual strain after five dry and ten wet thermal heating cycles
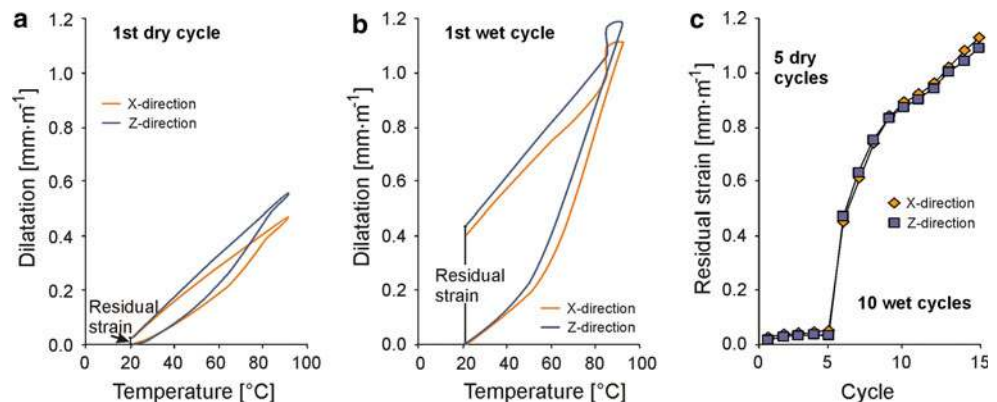
(Everett 1961). This mechanism is also defined by the curve of the length change measurements. At equilibration at about −19°C, a successive contraction of the sample is detectable. This frost shrinking can be traced back to a reduction of moisture swelling in combination with pressure solution of existing ice crystals. However, only a slight residual strain occurs within this experiment.

The Knaupsholz Granite only exhibits a very slight loss of weight during the freeze–thaw test. But a clear decrease of V_p and of the Young's modulus is detectable. The granite represents a slight to medium weathered rock. This is shown by the relatively high porosity of more than 1%. Fresh granites exhibit an effective porosity at about 0.2%. Furthermore, the rock shows a broad range of the pore radii distribution (Fig. 6d). This is possibly the cause for the length change behaviour during freezing of the water-saturated sample. Water first crystallises in larger pores, and enough unfrozen water in smaller pores is provided for ongoing crystallisation. This results in a strong expansion of the length change measurements, especially at about −19°C (Fig. 6l). By returning to the initial temperature, a strong residual strain remains. Since the dilatation measurements only shows one freeze–thaw cycle, the damage of the material could only be caused by the long-term frost action test.

Different weathering processes also superimpose each other, which counts not only for the laboratory experiments but also for nature. Since the different weathering processes vary at the buildings and sculptures, the freeze–thaw tests only indicate the weathering resistance of the rocks in winter months to a limited extent.

For laboratory weathering tests, the general question is to what extent the results can be transferred to the rocks used for buildings. In this study, 1,400 freeze–thaw cycles were performed. Using the climate of Munich, for example, where an estimated 30 freeze–thaw cycles per year occur, the frost weathering was simulated for a period of over 46 years. For the example of the Habichtswald Tuff, this would mean that the material was strongly damaged after 35 years of exposure.

Besides the frequency of freeze–thaw cycles, the frost intensity should also play an important role. The frost intensity describes how long and to what extent the temperature falls below the 0°C transition. According Walder and Hallet (1985), most of the damage potential can be assumed for a temperature of −10°C. However, this temperature range is seldom reached in most areas of Central Europe.

A further important parameter is the moisture content of the rocks during freezing. In the tests, the freeze–thaw resistance for capillary water-saturated samples were simulated. At buildings, wet freeze–thaw events are rare because the rocks have to be moistened before freezing.

This may happen during driving rain or the melting of snow above the 0°C limit. For the area of Budapest, (Hungary) about four wet freeze–thaw cycles actually occur per year (Fig. 9, Grossi et al. 2007). With the assumption that four freeze–thaw events having a high damage potential attacks the Habichtswald tuff, the material will exhibit a strong deterioration after 260 years.

When considering the importance of laboratory test results for the resistance of the rocks, the relevance of climatic change also increases. After calculations by Grossi et al. (2007), many regions in Central Europe will show a
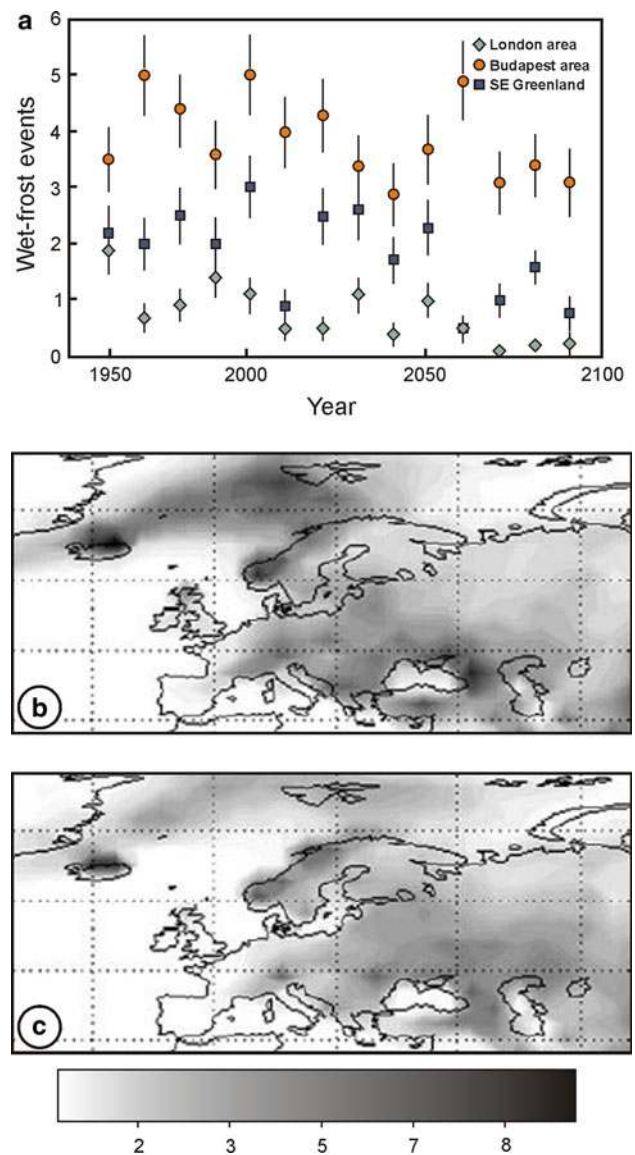

Fig. 9 Decadal means of wet frost events in the areas around central England, Hungary and South East Greenland. **a** The numbers of events tend to decrease. Pan-European maps of annual frequency of wet-frost events for **b** base line period (1961–1990) and **c** far future (2070–2099) modified after Grossi et al. (2007)

decrease in the frequency of freeze–thaw events (Fig. 9). However, in other areas which are characterised by long permafrost phases in winter, e.g. northern Europe, the frequency of freeze–thaw events will increase.

Conclusion

Freeze–thaw weathering of rocks is an important physical decay process at buildings. The freeze–thaw action test represents the standard method for evaluating the durability of a rock against the stresses induced by ice crystallisation in the pore spaces. The investigations in this work show that the results of the freeze–thaw action test leads to a comprehensive interpretation of the evaluated data, but only when further methods and other weathering mechanisms are taken into consideration. The following issues should be accounted for:

- Rapid tests of less than 50 action cycles allows in most cases only limited evidence about the real freeze–thaw sensibility of a natural building stone.
- The pure acquisition of the weight change after the freeze–thaw cycle is not sufficient to characterise the real fabric decohesion.
- Measurements of the compressional wave velocities are a useful tool for analysing the fabric decay during the frost action test. The measurement of the Young's modulus provided no further information about the damage process.
- For standard tests like the freeze–thaw action test, it is necessary to consider other decay processes like the moisture expansion or thermal dilatation, which can be affected by the test and can represent the more effective mechanism of material damaging during the weathering simulation.

References

Chahall RS, Miller RD (1965) Supercooling of water in glass capillaries. Br J Appl Phys 16:231–239

Correns CW, Steinborn W (1939) Über die Erklärung der sogenannten Kristallisationskraft. Z Kristallogr 101:117–133

Everett DM (1961) The thermodynamics of frost damage to porous solids. Trans Faraday Soc 57:2205–2211

Fei Y (1995) Thermal expansion. In: Ahrens TJ (ed) Mineral physics and crystallography—a handbook of physical constants, pp 29–44

Fitzner B, Snethlage R (1982) Einfluß der Porenradienverteilung auf das Verwitterungsverhalten ausgewählter Sandsteine. Bautenschutz und Bausanierung 5(3):97–103

Grossi CM, Brimblecombe P, Harris I (2007) Predicting long term freeze-thaw risks on Europe built heritage and archaeological sites in a changing climate. Sci Total Environ 377:273–281

Hirschwald J (1908) Die Prüfung der natürlichen Bausteine auf ihre Verwitterungsbeständigkeit. Verlag Wilhelm Ernst & Sohn, Berlin

Koch A, Siegesmund S (2001) Gesteinstechnische Eigenschaften ausgewählter Bausandsteine. Z Deut Geol Ges 152:681–700

Nicholson DT, Nicholson FH (2000) Physical deterioration of sedimentary rocks subjected to experimental freezing and thawing. Earth Surf Process Landf 25:1295–1307

Poschlod K (1989) Das Wasser im Porenraum kristalliner Naturwerksteine und sein Einfluß auf die Verwitterung. Münchner Geowissenschaftliche Abhandlungen 7:62 S

Powers TW, Helmuth RA (1953) Theory of volume changes in hardened Portland cement paste during freezing. Highw Res Board Proc 32:285–297

Rentsch W, Krompholz G (1961) Zur Bestimmung elastischer Konstanten durch Schallgeschwindigkeitsmessungen. Fachzeitschrift der Bergakademie Freiberg 7–8:492–504

Ruedrich J, Siegesmund S (2006) Fabric dependence of length change behaviour induced by ice crystallisation in the pore space of natural building stones. In: Fort R, Alvarez de Buergo M, Gomez-Heras M, Vazquez-Calvo C (eds) Heritage, weathering and conservation, vol 1, pp 497–505

Ruedrich J, Siegesmund S (2007) Salt and ice crystallisation in porous sandstones. In: Siegesmund S, Steiger M (eds) Salt decay. Environ Geol 52:225–249

Scherer GW (1999) Crystallization in pores. Cem Concr Res 29:1347–1358

Setzer MJ (1999) Mikroeislinsenbildung und Frostschaden. Eiligehausen R. (Hrsg.): Werkstoffe im Bauwesen—Theorie und Praxis (Construction materials—theory and application). Ibidem Stuttgart, pp 397–413

Siegesmund S, Ruedrich J (2008) Marble bowing. In: Proceedings 11th international congress on deterioration and conservation of stone, Torun, Poland

Siegesmund S, Ruedrich J, Koch A (2008) Marble bowing: comparative studies of three different public building facades. Environ Geol. doi:10.1007/s00254-008-1307-z

Snethlage R (1984) Steinkonservierung. Bayerisches Landesamt für Denkmalpflege. Arbeitshefte 22:203

Steiger M (2005) Crystal growth in porous materials. I: The crystallisation pressure of large crystals. J Cryst Growth 282:455–469

Stockhausen N (1981) Die Dilatation hochporöser Festkörper bei Wasseraufnahme und Eisbildung. Ph.D. TU München, p 163

Thomachot C, Jeanette D (2002) Evolution of the petrophysical properties of two types of Alsatian sandstone subjected to simulated freeze-thaw conditions. In: Siegesmund S, Weiss T, Vollbrecht A (eds) Natural Stone, Weathering Phenomena, Conservation Strategies and Case Studies. Geological Society, London, Special Publication No. 205, pp 19–32

Thomachot C, Matsuoka N (2007) Dilation of building materials submitted to frost action. In: Přikryl R, Smith BJ (eds) Building stone decay: from diagnosis to conservation. Geological Society, London, Special Publication No. 271, pp 167–177

van Brakel J, Modry S, Svata M (1981) Mercury porosimetry: state of the art. Powder Technol 29:1–12

Walder J, Hallet B (1985) A theoretical model of the fracture of rock during freezing. Geol Soc Am Bull 96:336–346

Weiss G (1992) Die Eis und Salzkristallisation im Porenraum von Sandsteinen und ihre Auswirkung auf das Gefüge unter besonderer Berücksichtigung gesteinsspezifischer Parameter. Münchner Geowissenschaftliche Abhandlungen, Reihe Band 9:S62

Winkler EM (1968) Frost damage to stone and concrete: geological considerations. Eng Geol 2:315–323